INTERIM REPORT
Submitted to the Exxon Valdez Trustee Council

Project: Pilot Studies of Bioremediation of the *Exxon Valdez* Oil in Prince William Sound Beaches

Michel C. Boufadel, PhD, PE, Brian A. Wrenn, PhD,

Center for Natural Resources Development and Protection
Department of Civil & Environmental Engineering
Temple University
Philadelphia, PA 19122

Exxon Valdez Trustee Council
Project No. 11100836

Introduction

The 1989 *Exxon Valdez* oil spill polluted around 800 km of intertidal shorelines within Prince William Sound (PWS), Alaska (Neff and Stubblefield, 1995; Neff et al., 1995). Studies conducted by scientists from the National Oceanic and Atmospheric Administration (NOAA) estimated that between 60 and 100 tons of subsurface oil persists in many initially-polluted beaches in Prince William Sound (PWS) (Short et al., 2004; Short et al., 2006). The persistence of oil was also noted by other studies (Hayes and Michel, 1999; Michel and Hayes, 1999; Page et al., 2008; Taylor and Reimer, 2008; Li and Boufadel, 2010). The lingering oil contains relatively high concentrations of polycyclic aromatic hydrocarbons (PAH; Short et al., 2004), which are known to be toxic to intertidal organisms (Carls et al., 2001), and sea otters and harlequin ducks may be exposed to subsurface lingering oil while foraging on the beaches of northern Knight Island (Short et al., 2006).

Previous research showed that the persistence of oil from the *Exxon Valdez* oil spill was correlated with specific geomorphic and hydrological characteristics of the beaches, and a probabilistic model of the distribution of lingering oil was developed (Michel et al., 2010). By investigating five beaches that are contaminated with moderate to heavy oil residue (MOR to HOR), Temple University scientists showed that contaminated beaches consist of an upper high-permeability layer that is underlain by a lower layer that is two to three orders of magnitude less permeable (Li and Boufadel, 2010; Bobo et al., 2010; Xia et al., 2010; Guo et al., 2010). On these beaches, the lingering *Exxon Valdez* oil was located a few inches (0.10 m) below the interface of the two layers (Fig. 1). Oil-contaminated sediments were anoxic (DO < 1 mg/L and low nitrate concentration), whereas similar oil-free sediments were oxic (DO > 3 mg/L and high nitrate concentrations), suggesting that oil biodegradation may be oxygen limited in sediments that are contaminated with lingering oil. In addition, the concentrations of available nutrients in contaminated sediments (<0.5 mg N/L; <0.04 mg P/L; Boufadel et al., 2010; Sharifi et al., 2011) were lower than the concentrations that are required to support maximal rates of oil biodegradation ($\geq$ 2 mg N/L and N:P ratio of about 10:1; Atlas and Bartha, 1973; Venosa et al., 1996; Smith et al., 1998; Boufadel et al., 1999; Du et al., 1999; Garcia-Blanco, 2004). Although some have suggested that the poor biodegradability is responsible for persistence of the lingering oil in Prince William Sound shoreline sediments (Atlas and Bragg, 2009a,b), a recent study

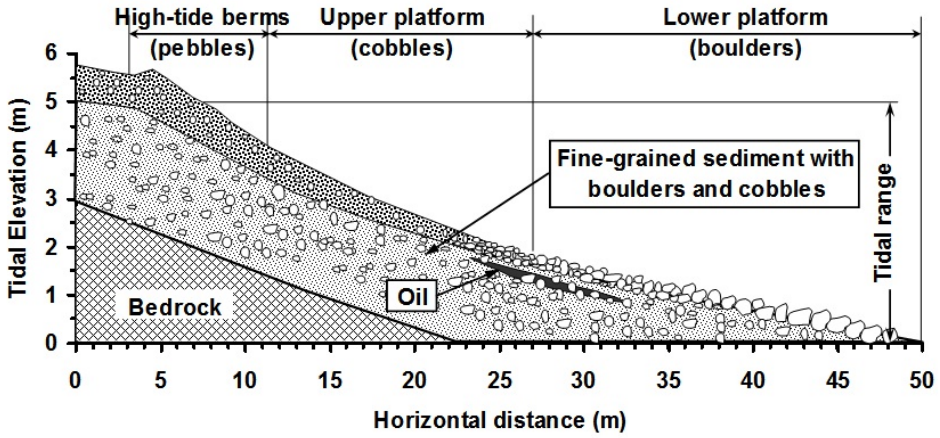

Figure 1: Persistence of oil in the lower layer of beaches in Prince William Sound. (From Li and Boufadel, 2010; Copyright Nature Publishing Group).

showed that this was not the case, and that even highly weathered oil was amenable to extensive biodegradation (Venosa et al., 2010). Therefore, this study was conducted to determine whether bioremediation of lingering oil could be stimulated by injection of nutrients into the contaminated subsurface.

Sites

The locations of four beaches used in this study are shown in Figure 2: EL056C (Northwest

Figure 2: Locations of beaches used for bioremediation pilot studies.

Bay on Eleanor Island; 60°33'45.6"N/147°34'17.4"W), SM006B (Smith Island; 60°32'39.1"N/147°23'6.4"W), PWS3A44 (Mears Point, Perry Island; 60°39'24.2"N/147°55'54.8"W), and LA015E (Latouche Island; 60°03'34.7"N/147°49'01.7"W). Two of the beaches (EL056C and SM006B) were used in a previous Temple University study to investigate hydrodynamic limitations of the oil bioremediation rate.

Bioremediation Approach

With the exception of the zone near the high tide line, the net movement of pore water applied onto the beach surface is seaward in any beach subjected to tide (Boufadel et al., 2006, Li et al., 2007, Brovelli et al., 2007). Therefore, solutions applied onto the beach surface would tend to be washed out to sea. Due to the two-layer structure of contaminated beaches in PWS, where the upper layer has a permeability that is 100 to 1,000 times that of the lower layer, solutions applied onto the surface tend to dilute and wash out to sea much more rapidly than they can be transported into the contaminated layer. This was described by Xia et al. (2010), who found—based upon numerical simulations using hydraulic characteristics measured at a contaminated beach—that the nutrient concentration in the oil-contaminated sediments would be only 1% of the concentration applied to the beach surface. Therefore it is unlikely that surface application of nutrients would be effective except in situations where the oil layer is very shallow and the nutrient solution is applied directly to the oil patch. Direct injection of a conservative tracer into the lower layer of two-layer beaches, on the other hand, resulted in much less dilution (Bobo et al., in press). Therefore, subsurface delivery of nutrients was expected to be superior to surface application and was selected for use in this study.

Nutrients were injected into the lower layer using one of two injection methods: high pressure injection (HPI) and ambient pressure release (APR). HPI is intended for use on beaches for which the depth to bedrock is greater than one meter, whereas APR is intended for use on beaches for which 0.8 m or less of sediments overlie bedrock. For the purpose of this study, the depth to "bedrock" was considered to be the depth to which a pit could be dug. This depth was often limited by the presence of a layer of boulders rather than true bedrock. The HPI injection method was used at EL056C and involved a single row of three injection wells spaced at 2-m intervals (Fig. 3). The APR method was used at SM006B, PWS3A44, and LA015E, and it used two rows of four injection wells spaced about one meter from each other (Fig. 4). The design flow rate for HPI was 1.0 L/min/well, and the design flow rate for APR was 0.2 L/min/well.

The injection wells were constructed using 2-in PVC pipe with 1-ft prepack well screens. The bottoms of the injection wells at EL056C were at depths ranging from 1.0 m (I-R) to 1.3 m (I-L) below the beach surface. The depth of injection well I-R was limited by a large subsurface boulder or bedrock at the well location; the depth of well I-L was limited by a clay layer beginning at a depth of about one meter below the beach surface. A cross-sectional diagram of the injection wells at EL056C is shown in Figure 5. The bottoms of the injection wells installed at SM006B were at depths ranging from 0.8 m to 0.9 m below the beach surface, and the well screens were horizontal to the beach surface (Fig. 6). The wells at PWS3A44 were installed to a depth of about 0.8 m, and the screens were installed vertically (Fig. 7). The wells at LA015E were installed to depths ranging from 0.6 to 0.8 m below the beach surface, but the well screens were horizontal to the beach surface (Fig. 8).

Nutrients were pumped into the injection wells using a 24-VDC diaphragm pump (Shurflo Model No. 800-151-296), and the flow was controlled using rotameters equipped with needle

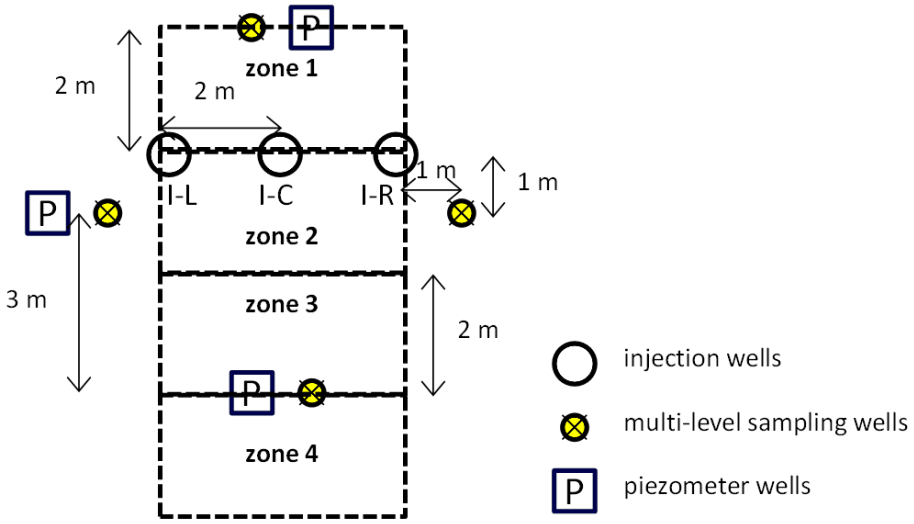

Figure 3: Plot layout for the high-pressure injection (HPI) system that was used at EL056C. The top of the diagram corresponds to the landward direction and the bottom is seaward. Sediment samples were collected from predetermined locations within zones 1-4.

valves (Dwyer Instruments, Model No. RMB-83D-SSV). Every injection well at EL056C and SM006B was connected to its own rotameter, but the injection wells installed at PWS3A44 and LA015E were connected to manifolds (one manifold for each row of four wells; see Figs. 7 and 8). So, the flow rates were controlled separately to each well at EL056C and SM006B, but they were controlled to a row of injection wells at PWS3A44 and LA015E. The injection pump, rotameters, nutrient solutions, and other power, control, and pumping equipment were installed in small wooden buildings that were placed on each beach. The nutrient solutions—hydrogen peroxide, lithium nitrate, and sodium tripolyphosphate (STPP)—were injected into flowing seawater using 12-VDC metering pumps (LMI Milton Roy, Model No. JD54D). The seawater was collected from the lower intertidal zone of the beach being treated during high tides and stored in a 1500-gal tank next to the treatment building.

Hydrogen peroxide was provided as the source of oxygen for this study because it is an efficient, water-soluble oxygen source that decomposes to oxygen and water as the only products (Pardieck et al., 1992). Hydrogen peroxide has been widely used to provide oxygen to support bioremediation of hydrocarbon-contaminated groundwater and subsurface sediments (Pardieck et al., 1992). Although hydrogen peroxide decomposition can be catalyzed by common minerals and enzymes that are likely to be present in the beach subsurface, it is reasonably stable in the absence of sediments (Lawes, 1990). Hydrogen peroxide was provided as a concentrated (35%, w/w) solution. A concentrated nutrient solution was prepared by dissolving lithium nitrate and STPP in freshwater to concentrations of 100 g $LiNO_3$/L and 8 g STPP/L.

The injected concentrations of nutrients were: 100 mg/L as hydrogen peroxide, 20 mg N/L as lithium nitrate ($LiNO_3$), and 2 mg P/L as STPP ($Na_5P_3O_{10}$). The concentration of nitrate that was used should be sufficient to support high rates of hydrocarbon biodegradation, and the N:P ratio has been shown to support rapid biodegradation of phenanthrene (Smith et al., 1998;

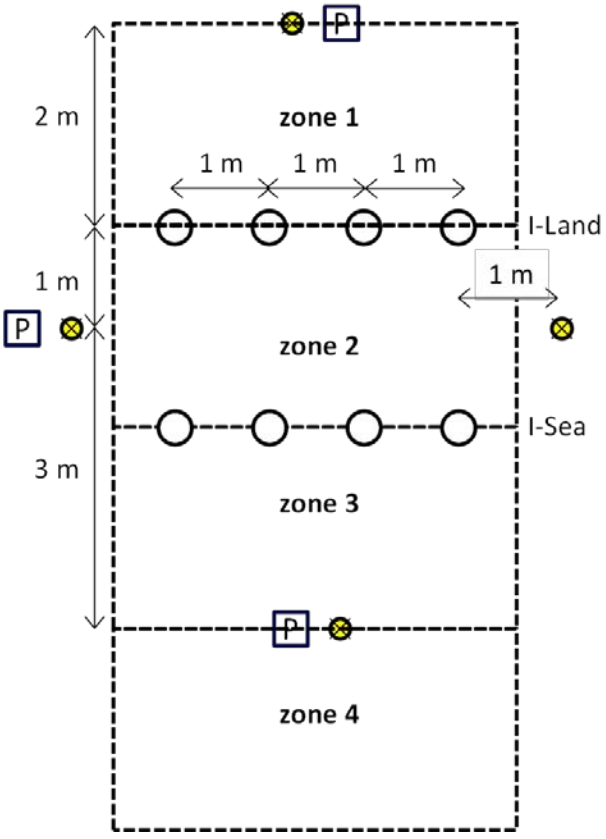

Figure 4: Plot layout for the ambient-pressure release (APR) systems that were used at SM006B, PWS3A44, and LA015E. I-Land and I-Sea indicate the landward and seaward rows of injection wells, respectively. Symbols have the same meaning as those used in Figure 3.

Garcia-Blanco, 2004). The hydrogen peroxide concentration was limited by the maximum solubility of oxygen in seawater (about 40 mg/L at 15 ^{o}C; Metcalf and Eddy, 1991): higher concentrations could lead to the formation of bubbles of oxygen gas that could reduce the permeability of the formation (Spain et al., 1989; Fiorenza and Ward, 1997). The lithium that was provided with lithium nitrate was used as a conservative tracer to estimate the amount of dilution that occurred due to turbulent diffusion and mixing with seawater (from tides) or freshwater (from infiltration of rain or seaward flow of groundwater).

Sample Collection and Analysis

Performance of the bioremediation systems was monitored using sediment samples and groundwater samples. Sediment samples were collected from each of the four 2-m by 4-m treatment zones that are shown in Figures 3 and 4. Two samples were collected from predetermined locations in each treatment zone three times during the project. The initial (i.e., pretreatment) samples were collected after the injection wells were installed but before the systems were turned on, and the posttreatment samples were collected after the systems had been operating for about one (August) and two (September) months. Sediment samples were collected by digging pits at the predetermined locations to depths of about 0.6 m below the

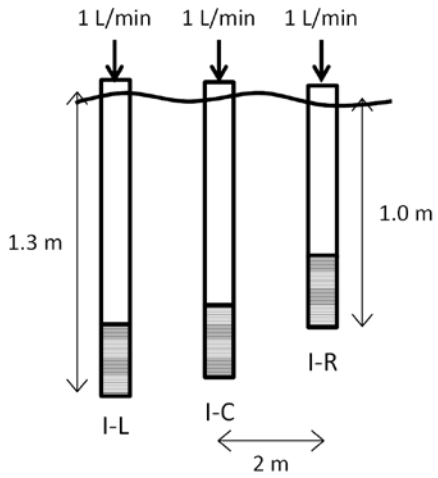

Figure 5: Injection wells at EL056C

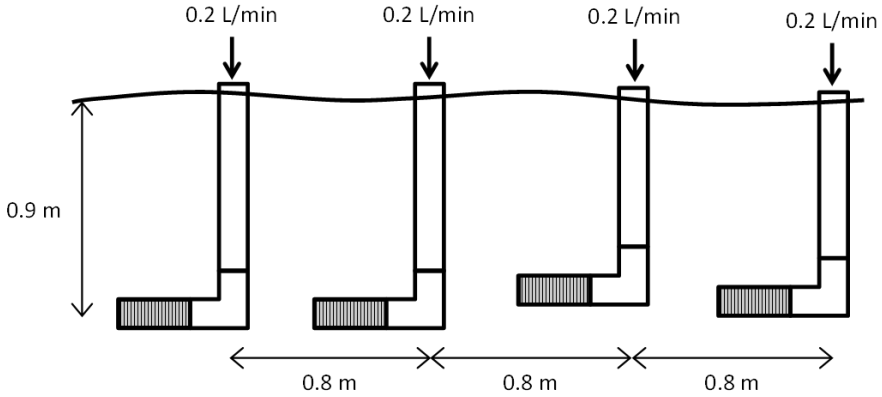

Figure 6: Injection wells at SM006B

ground surface or to the maximum depth that could be achieved, whichever was deeper. The depth of maximum oil contamination was identified visually, and sediment samples were collected from the walls of the pit. Separate samples were collected for analysis of oil, microbial community composition, and nutrients. Oil samples were collected in 125-ml glass sample bottles that had been cleaned according to EPA procedure 1 for semivolatiles. Oil samples were frozen as soon as practical after collection, and they were kept frozen during storage and shipment. Oil samples were analyzed by NOAA's Auke Bay Lab using GC-MS and Iatroscan. The microbiology samples were collected using aseptic technique (e.g., sterile sample containers, alcohol-rinsed and flamed spatulas, alcohol-rinsed vinyl gloves), and sediments were processed as soon as possible, usually within a few hours. (In two cases, several days elapsed between when the samples were collected and when they were processed. In those cases, the samples were refrigerated until they could be processed.) The composition of the microbial community was characterized by enumerating heterotrophic bacteria, alkane-degrading bacteria, and PAH-degrading bacteria using 96-well plate most-probable-number (MPN) procedures (Wrenn and Venosa, 1996).

Water samples were collected from multilevel sample wells, which were installed at the locations shown in Figures 3 and 4, and single-level wells, which were installed at the locations

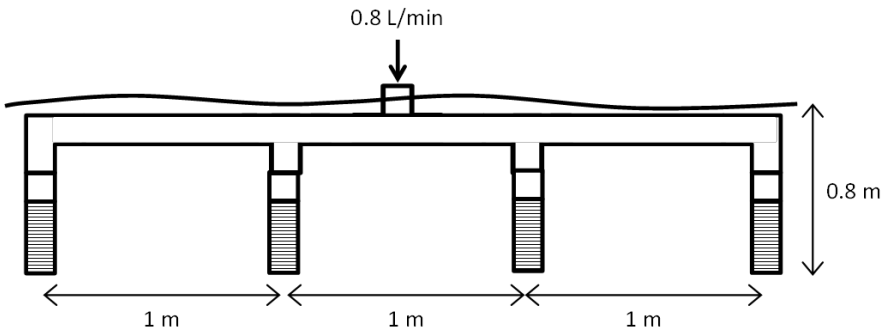

Figure 7: Injection wells at PWS3A44

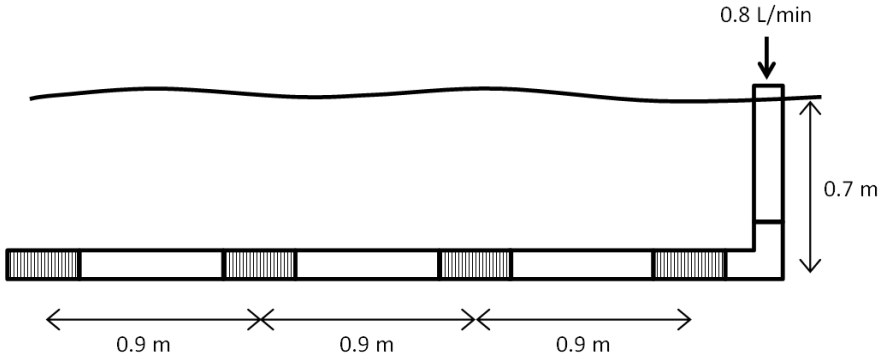

Figure 8: Injection wells at LA015E

from which the initial sediment samples were collected. The multilevel wells had sample ports at several depths below the beach surface, and so, they provide a three-dimensional picture of the distribution of nutrients. The multilevel wells, however, were installed at the edges of the expected treatment zone. The single-level wells, on the other hand, were installed within the plots at the depth at which the maximum amount of oil was observed. Eight single-level wells were installed in each plot: two wells were installed in each of the four sediment-sampling zones (Figs. 3 and 4).

Water samples were collected using disposable 60-ml polypropylene syringes (Becton Dickinson, Franklin Lakes, NJ) and used for measurement of nutrients, lithium (conservative tracer), and dissolved oxygen. The sample-collection procedure involved purging the wells by filling the syringe twice and discarding the water. The syringes were filled a third time, and the water was used to rinse the 125-ml polyethylene sample bottle. (The sample bottles were acid washed, rinsed with deionized water, and air dried before use.) The fourth syringe volume was the nutrients sample. Nutrient samples were frozen as soon as possible, and kept frozen during storage and shipment. Each syringe was filled one more time and then sealed by closing a two-way valve. The fifth syringe volume was used to measure the dissolved oxygen concentration using the Hach High-Range DO assay (Hach Company, Loveland, CO). The DO samples were analyzed as soon as possible after collection, usually within about 2-3 hours of being collected.

Nutrients were measured colorimetrically using an AutoAnalyzer3 (Seal Analytical, Mequon, WI; Grasshoff et al., 1999). The frozen samples were defrosted and stored at 4 °C until they were analyzed. Before analysis, the samples were shaken by hand for 15 s, and filtered through 0.45-μm PTFE membrane filters (Puradisc,Whatman, Florham, NJ) into the

AutoAnalyzer3 cups. Ammonia in seawater was measured using the Berthelot reaction, and the colored reaction product was measured at 660 nm. Nitrate in the samples was reduced to nitrite by a copper-cadmium reactor column, and the nitrite reacted with sulfanilamide under acid condition to form a purple azo dye that was analyzed at 550 nm. Phosphate was measured using the ascorbate-antimony-molybdate method (Murphy and Riley, 1962). The blue complex was analyzed at 880 nm wavelength. The lithium concentration was measured using atomic absorbance spectrometry (AAS).

Results

Startup and Operation:

The bioremediation pilot-scale test plots were set up from May 23-June 8, 2011. This included installation of the injection and monitoring wells, construction of the buildings that housed the power and control equipment, connection of the pumps to the wells, and installation of the seawater-intake pumps and storage tanks. Due to delays in permitting, the systems installed at the three sites located in the Chugach National Forest (EL056C, SM006B, and PWS3A44) were not turned on immediately. Instead, Temple University received permission to install the bioremediation systems but not to turn them on. The permit was issued on June 28, but due to the generator issues described below, the systems were not started for another three weeks (PWS3A44, July 19, 2011; EL056C and SM006B, July 21, 2011).

The system at LA015E was located on property owned by the Chenega Corporation. Because the permit for this site was obtained before beginning work, system operation began immediately after installation (May 29, 2011). Unfortunately, the generator that was used to charge the batteries burned out almost immediately (discovered on June 6 and replaced on June 9). The second generator also burned out within a week of installation (discovered on June 16). We concluded that the problem was most likely due to overheating caused by the design of the boxes in which the generators were housed. The generator boxes were redesigned and rebuilt, and no further generator problems occurred. The system at LA015E was restarted on July 6, 2011.

Weather and equipment problems caused system shutdowns at all four sites at some time during the course of the study. So, the results reported here reflect a much shorter treatment time than was originally envisioned (about 6 weeks of actual operation vs. 12 weeks planned). For example, storm damage was discovered at PWS3A44 on August 7 and the system was repaired and restarted by August 10. All of the systems had been damaged by storms prior to collecting the last samples (i.e., between September 8 and September 14). This damage probably occurred during severe storms that occurred during the first week of September.

Oil Degradation:

Sediment samples were collected from two locations in each of four zones (Figs. 3 and 4) three times during this study: immediately after installing the injection wells (initial), about 3 weeks after starting the bioremediation systems (August), and about 7 weeks after system startup (September). The total concentration of oil in every sample was estimated based on the mass of oil extracted, and the average concentrations measured in each zone at the four sites are shown in Figure 9. These data show that the average concentration of oil was highest at SM006B (5.9 $\pm$ 7.1 g oil/kg sediment) followed by EL056C (3.6 $\pm$ 3.8 g oil/kg sediment). Substantially lower concentrations were observed at LA015E (1.2 $\pm$ 1.2 g oil/kg sediment) and PWS3A44 (0.7 $\pm$ 0.9

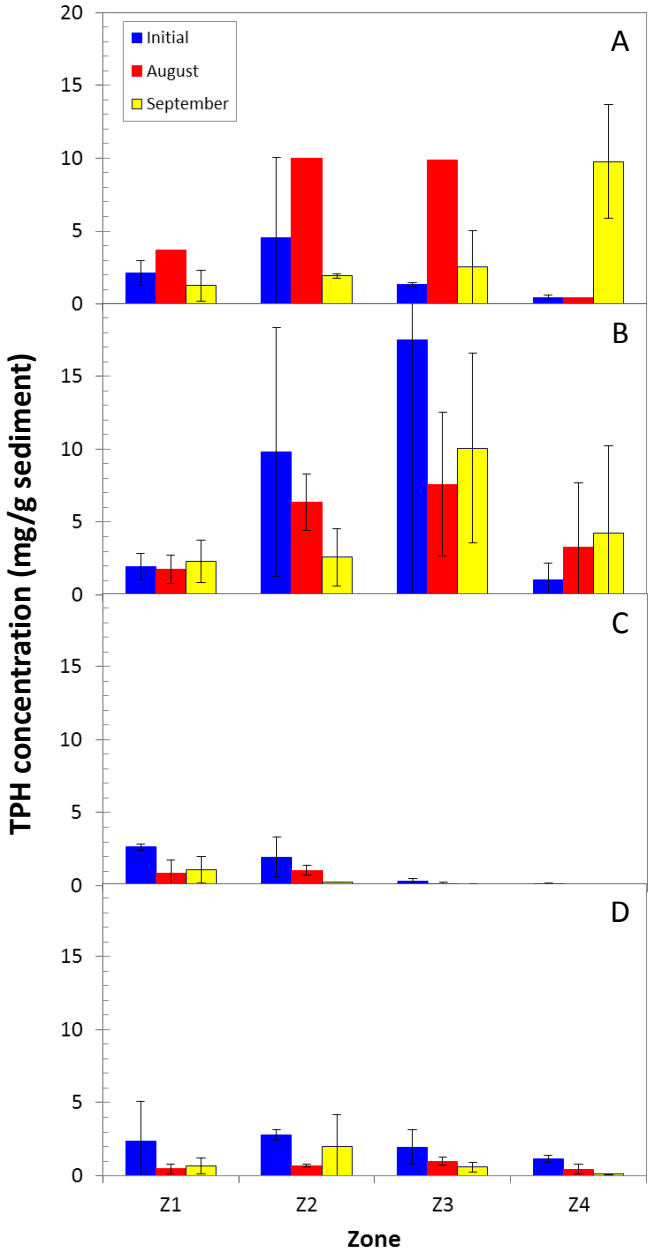

Figure 9: Average oil concentrations observed at (A) ELO56C, (B) SM006B, (C) PWS3A44, and (D) LA015E during the pilot-scale bioremediation study. Z1, Z2, Z3, and Z4 refer to the zones shown in Figs. 3 and 4.

g oil/kg sediment). As the standard deviations reported above and the data shown in Figure 9 suggest, the observed total oil concentrations varied from sample to sample, probably due to the patchy nature of the residual oil and the relatively small sample size (about 100 g). This variability would have made it difficult to identify significant treatment effects based on total oil concentration. Also, much of the concern regarding the lingering effects of oil can be attributed to the polycyclic aromatic hydrocarbons (PAH) that are present because these compounds can be toxic, mutagenic, and bioaccumulative. Therefore, the data were analyzed by first normalizing

the observed PAH concentrations using the observed concentration of C2-chrysene, which has been shown to be lost slowly relative to other PAHs in artificial weathering studies (Short and Heintz, 1997). This normalization procedure allows changes in the concentrations of components of interest to be evaluated without confounding due to variability of the concentration of oil in the sample.

In addition to the quasi-random variability that was observed in the oil concentration data, the oil observed in samples collected from the far-left side of the plot at EL056C (nodes 12 and 24) appeared to be more weathered than was the oil in samples collected from the center-and-right side of the plot (nodes 4, 11, 19, 28, and 31; Fig. 10). The data shown in Fig. 10 is presented as the sum of the concentrations of 48 PAH that were measured by GC-MS, and the

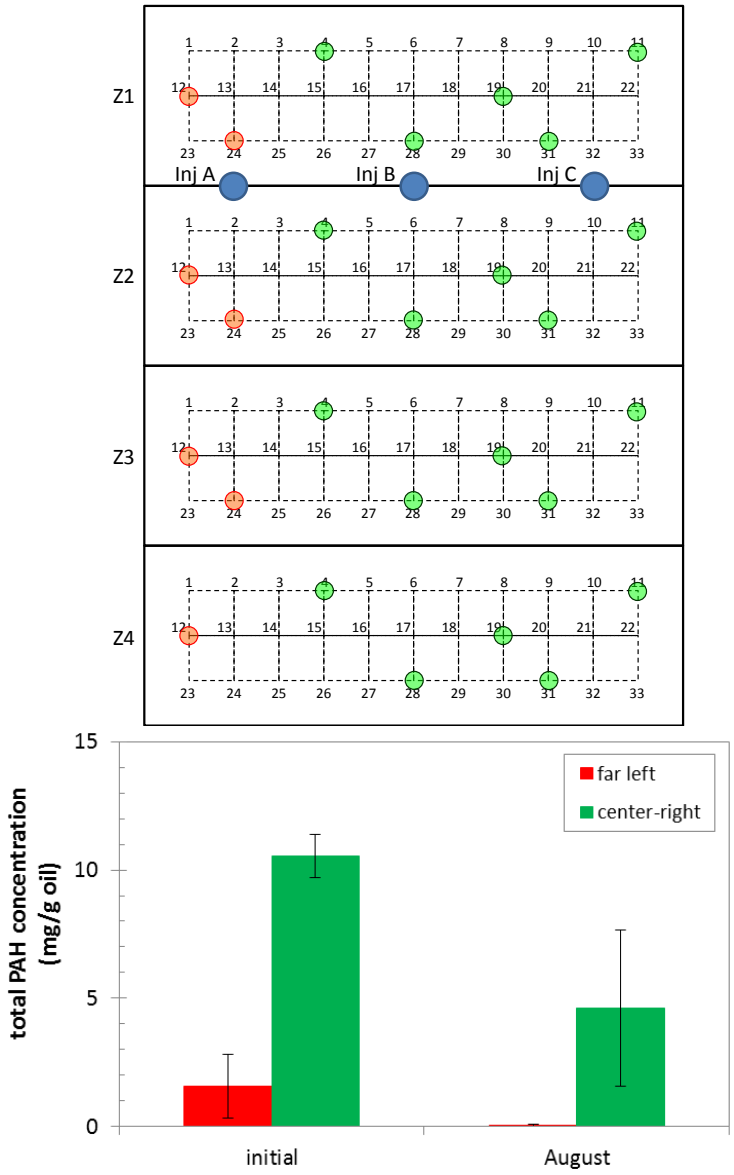

Figure 10: Top: location of sediment samples collected at EL056C; Bottom: average total PAH concentrations observed in May ("initial") and August 2011.

concentrations were normalized to the gravimetric oil concentration rather than to the concentration of C2-chrysene. C2-chrysene normalization was not used in this analysis because the C2-chrysene concentration was below the method detection limit in three of the seven samples collected from the left side of the plot. Figure 10 shows that the total concentration of PAH was smaller on the far left side of the plot than in the rest of the plot at both time points ($P = 0.0002$, where P is the probability that the total PAH concentration was the same at both locations; $P = 1$ indicates 100% probability that the concentrations at the two locations were the same). Note that normalization of the PAH concentrations to C2-chrysene instead of TPH did not change this conclusion, but due to the smaller number of samples available for the left side of the plot, the probability that the concentrations were the same at both locations increased to 0.002 (0.2% probability that the average concentrations were the same). Note that the concentrations of important components (esp., dissolved oxygen and salinity) were significantly different in initial groundwater samples collected from the multiport well on the left side of the plot and those collected at other locations (Table 1). Most importantly, the salinity was much lower on the far-left side of the plot and the dissolved oxygen was much higher, suggesting that the greater weathering observed on the far-left side of the plot may have been due to subsurface flow of freshwater from the stream on the left side of the beach. Because the oil in samples collected on the far-left side of the plot at EL056C was much more weathered than oil from the rest of the plot, those samples were treated separately in the following analysis.

Table 1: Groundwater characteristics at EL056C before bioremediation system startup

parameter	far left side	rest of plot
salinity (g/L)	3	27.1 ± 2.4
dissolved oxygen (mg/L)	7.5	2.1 ± 1.7
nitrate (mg N/L)	0.10	0.21 ± 0.25
ammonia (mg N/L)	0.04	0.18 ± 0.13

Biodegradation of lingering oil due to operation of the bioremediation systems at the four pilot-scale test sites is shown in Figures 11 and 12. The significance of observed changes in the total normalized PAH concentrations were analyzed using two-way analysis of variance (ANOVA) treating each site separately. Time and treatment zone were used as the independent treatment factors. The criterion for rejecting the null hypothesis for any treatment effect or interaction was set at $P = 0.013$ for each site to maintain a global Type 1 error rate of 5%. When significant treatment effects were identified, Tukey's Honestly Significant Difference (HSD) was used to identify means that were significantly different. Time effects were only compared within specific treatment zones (i.e., the concentration observed in zone Z2 at EL056C in August was compared to the initial concentration in Z2 but not to the initial concentrations in zones Z1, Z3, or Z4).

Figure 11 shows the plot average C2-chrysene-normalized total PAH concentration before system startup (initial), after three weeks of operation (August), and about 7 weeks after startup (September). The normalized plot average concentrations decreased significantly from the initial values at EL056C and PWS3A44 ($P < 0.05$) but were unchanged at SM006B and LA015E. At both locations exhibiting significant biodegradation, the biggest change occurred shortly after

system startup. Note that, although four weeks elapsed between the August and September samples, none of the bioremediation systems were operational when the final samples were collected due to storm damage that is thought to have occurred during the first week of September.

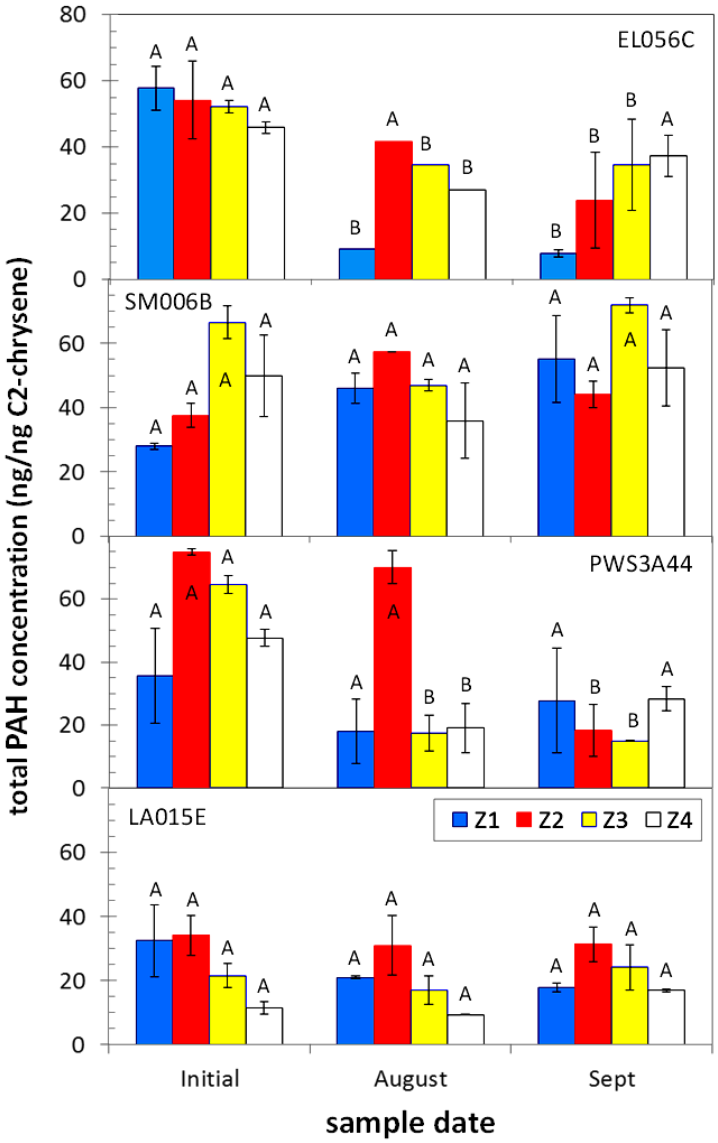

Figure 12: Concentrations of total PAH normalized to the concentration of C2-chrysene in the four treatment zones at the beaches at which pilot-scale bioremediation was tested. Bars labeled with the same letter are not significantly different from each other. Values are compared only within a specific site and treatment zone.

the initial concentration. Bars labeled with the same letter are not significantly different from each other. Values are compared only within a specific site.

Figure 12 shows the performance in each treatment zone as a function of time. For the beaches at which significant treatment effects were observed (i.e., EL056C and PWS3A44), significant effects were more likely to be observed close to the injection wells than far from them. The absence of consistent temporal trends in zone Z4 at both sites probably reflects patchiness and suggests that this was beyond the zone of influence of the injection wells. Significant treatment effects in zone Z1, which was landward of the injection wells, at EL056C,

is consistent with the results of a tracer study that was conducted at this site in 2009, which showed that a conservative tracer was observed within about 20 hours at a sample well located 1.6 m landward of an injection well that was operated using the high-pressure injection (HPI) method, as was used at EL056C in this study (Boufadel and Bobo, 2011). Treatment effects were not observed in zone Z1 at PWS3A44, which used the ambient pressure release (APR) injection method. A summary of the initial total normalized PAH concentrations and the removal percentages that were observed in each treatment zone is given in Table 2 for all of the pilot-scale bioremediation test sites.

Table 2: Normalized total PAH concentrations and removal percentages

Site	Zone	initial PAH_{tot} concentration (ng/ng C2-chrysene)	percentage reduction† August	percentage reduction† September
EL056C	Z1	57.8 ± 4.7	84%*	86%*
	Z2	54.2 ± 8.3	23%	56%*
	Z3	52.5 ± 1.4	34%*	34%*
	Z4	45.9 ± 1.2	41%*	19%
SM006B	Z1	28.0 ± 0.9	-64%	-97%
	Z2	37.6 ± 3.8	-52%	-17%
	Z3	66.6 ± 5.0	29%	-8%
	Z4	50.0 ± 12.7	28%	-5%
PWS3A44	Z1	25.6 ± 15.1	49%	22%
	Z2	74.9 ± 1.0	6%	76%*
	Z3	64.6 ± 2.9	73%*	77%*
	Z4	47.6 ± 2.7	60%*	40%
LA015E	Z1	32.4 ± 11.2	35%	45%
	Z2	34.1 ± 6.2	9%	8%
	Z3	21.5 ± 3.7	21%	-12%
	Z4	11.4 ± 2.0	18%	-48%

†positive reductions indicate that the concentration decreased relative to the initial values; negative reductions indicate that the concentration increased

*concentration changes are significant at the 95% confidence level

Nutrient Concentrations:

Water samples were collected from four stainless steel multiport sampling wells (MP-Land, MP-Left, MP-Right, and MP-Sea) that were located around the edges of the test plots (see Figs. 3 and 4) and eight single-point sampling wells at each site. Water samples were collected before system startup (initial) and about 3 weeks (August) and 7 weeks (September) after startup. As

noted previously, none of the systems were operating when the September samples were collected due to storm damage. The water samples were frozen and shipped overnight to Philadelphia where the nutrient concentrations (nitrite/nitrate, ammonia, phosphate) were measured. Additional water samples were collected and the dissolved oxygen (DO) concentration was measured on site.

The measured dissolved oxygen concentrations are shown in Figure 13 for all sample-well locations. The data for the multiport wells is shown as location averages (i.e., averaged over all depths), and the concentrations tended to be higher close to the surface. In addition, the data collected from the two single-point wells in each treatment zone was also averaged, and the variability in dissolved oxygen within a treatment zone (i.e., between the two single-point wells) was also relatively high. This variability could be due to preferential flow paths through the treatment zone or channeling of water from the beach surface to the well point. As a result, few statistically significant differences resulting from operation of the bioremediation system can be discerned. At some locations, high DO concentrations were observed in September, when the system was not operating, suggesting that the wells were influenced by surface seawater or freshwater flow from an oxygen rich freshwater source (e.g., stream or pond).

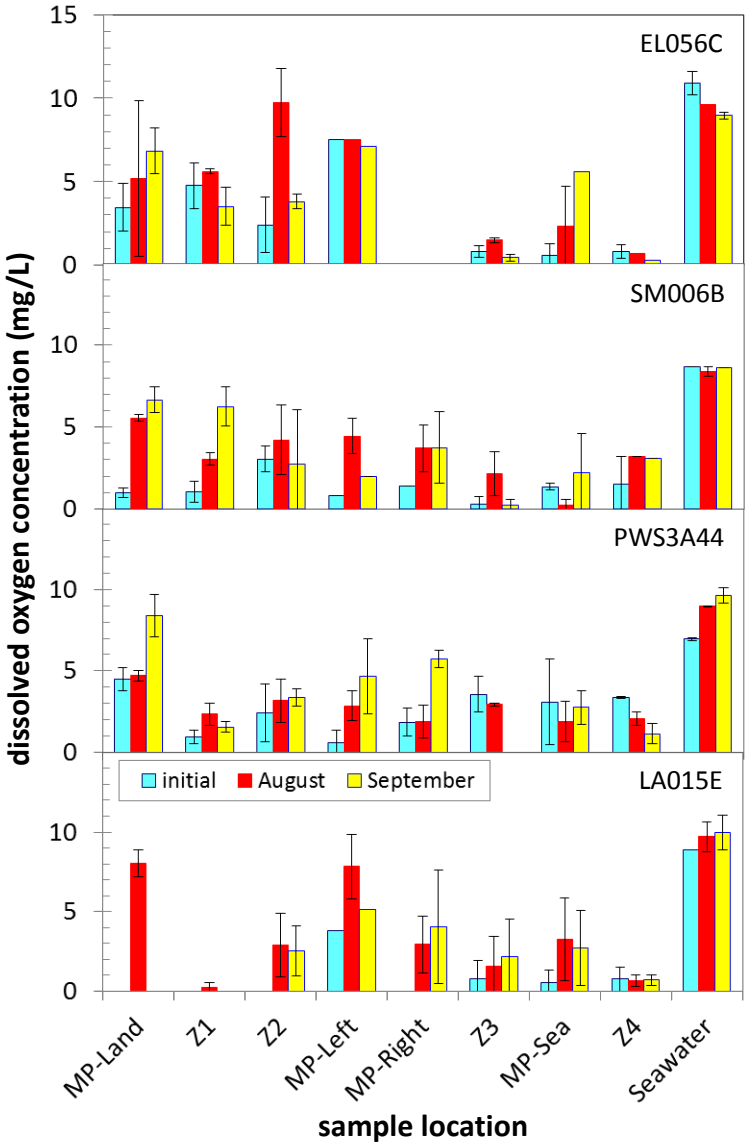

Figure 13: Dissolved oxygen concentrations observed at multiport (MP) and single-point wells at the bioremediation test sites. Sample locations on the left are most landward and on the right are most seaward.

The nutrient concentrations that were measured in pore water samples are shown in Figures 14 (nitrate), 15 (ammonia), and 16 (phosphate). As described above, nitrate and tripolyphosphate were injected into the subsurface in the treatment zone to stimulate bioremediation. At EL056C, the concentrations of nitrate measured in August—three weeks after starting nutrient injection—were higher than the background levels in treatment zones Z1 and Z2 and in multiport wells MP-Land and MP-Sea. The largest increase in the nitrate concentration occurred in Z2, which was just downgradient of the injection wells, and the amount of increase decreased with distance from the injection wells. Although it seems as if no increase was observed in treatment zone Z3 after starting nutrient injection, the relatively high concentration observed in that zone before starting the injection system was due to one sample location (Z3-4), whereas the second sample location in zone Z3 had an initial nitrate concentration that was more similar to other background concentrations. The smaller standard

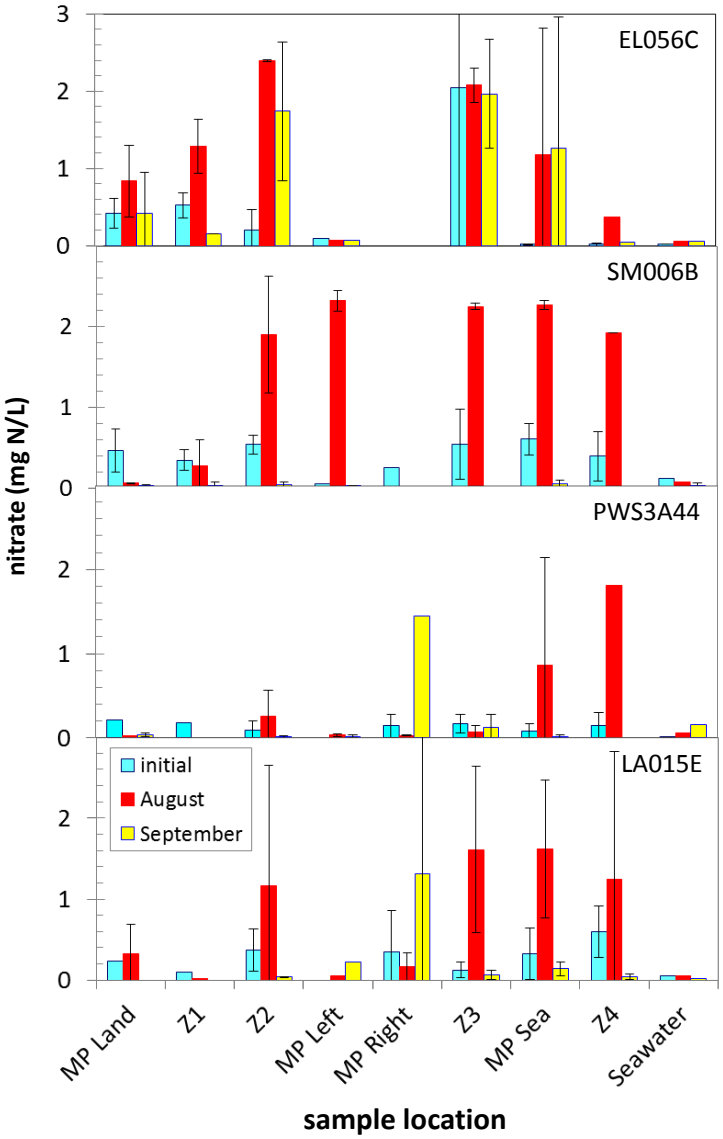

Figure 14: Nitrate concentrations observed at multiport (MP) and single-point wells at the bioremediation test sites. Sample locations on the left are most landward and on the right are most seaward.

deviation observed in August indicates that operation of the bioremediation system resulted in a more uniform distribution of nutrients. The relatively large error bars associated with samples collected from MP-Land and MP-Sea in August reflects higher concentrations near the beach surface at those locations. Surprisingly, the nutrient concentrations remained elevated in September at several locations downgradient of the injection wells at EL056C despite the fact that the injection system was not operating. This may reflect relatively slow washout of the nutrients from this part of the beach. (Note that we don't know when the bioremediation system stopped operating at this site. It could have been shortly before our arrival to collect samples.)

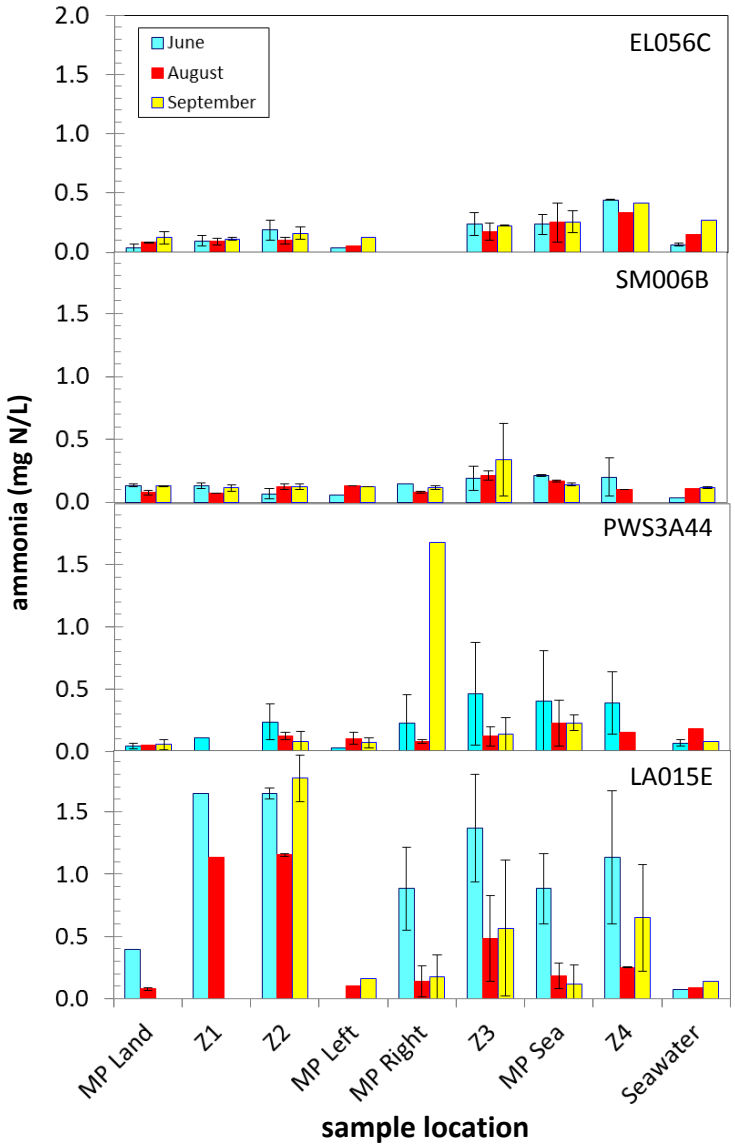

Figure 15: Ammonia concentrations observed at multiport (MP) and single-point wells at the bioremediation test sites. Sample locations on the left are most landward and on the right are most seaward. Note that ammonia was not added by the bioremediation system.

Higher nitrate concentrations were also observed downgradient of the injection wells at SM006B and LA015E in August. In general, the largest effects were observed relatively close to the injection wells (i.e., in zones Z2 and Z3 and at MP-Sea). A similar increase was not observed at PWS3A44, despite evidence of increased PAH biodegradation rate at this site. This difference almost certainly reflects the much higher groundwater flow rate that characterized this site.

The ammonia-nitrogen concentrations were not affected by operation of the bioremediation system. Note that the background concentrations of ammonia were significantly higher at LA015E, which had a relatively large amount of fine, organic-rich sediment mixed among the cobble and boulders. The hydraulic conductivity of LA015E was relatively low.

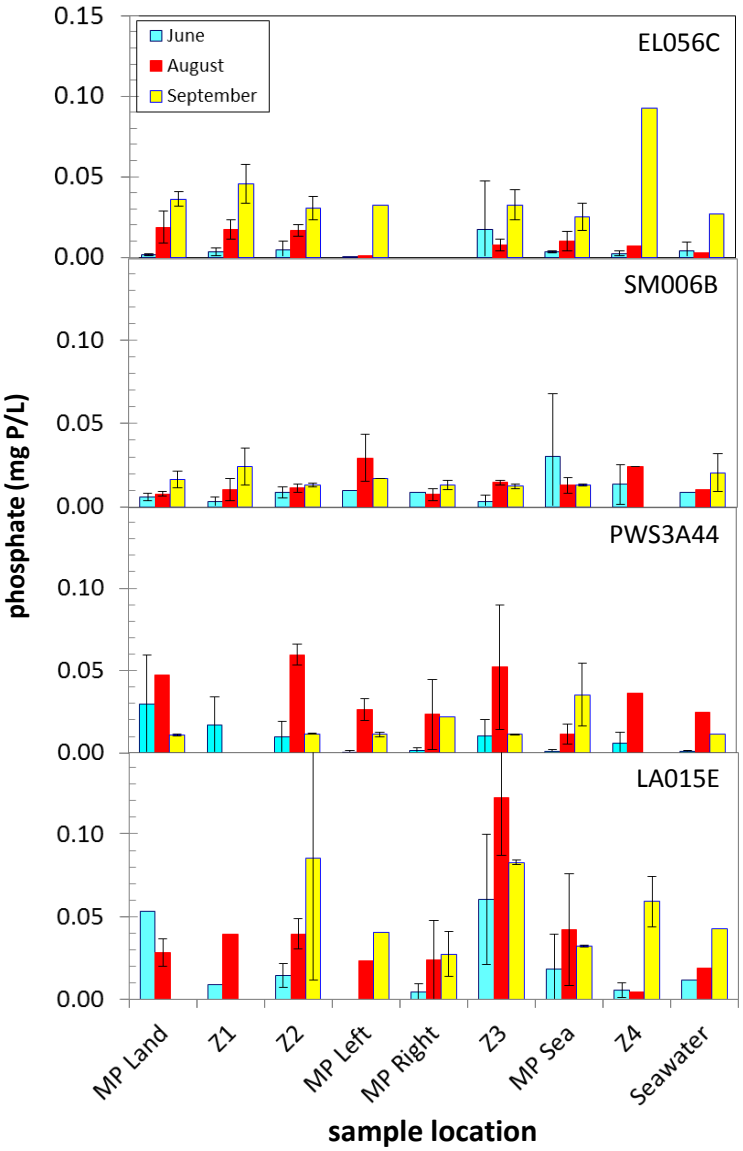

Figure 16: Phosphate concentrations observed at multiport (MP) and single-point wells at the bioremediation test sites. Sample locations on the left are most landward and on the right are most seaward.

Elevated phosphate concentrations were observed at EL065C, PWS3A44, and LA015E as a result of operation of the bioremediation systems. In general, phosphate transport was much slower than was transport of nitrate (i.e., the effects were observed only close to the injection wells), which is consistent with its lower solubility in seawater and greater tendency to adsorb to sediments. Phosphate concentration changes not observed at SM006B, probably reflecting stronger phosphate-binding capacity at this site. The phosphate concentrations observed in September at EL056C and LA015E remained high, and in some cases were higher than those observed in August. This may reflect either slow accumulation of phosphate due to the longer operation of the bioremediation system or release of phosphate from the sediments due to the sediment becoming anoxic with subsequent reduction of iron oxides in the sediments (iron oxides are known to strongly bind phosphates in sediments; Tiyapongpattana et al., 2004; Oxmann et al., 2008).

The salinity is shown in Figure 17. Although the salinity was not affected by operation of the bioremediation systems, it varied between sites and with location and time within a site. The relatively low salinity observed at PWS3A44 in August and September probably reflected the flow of fresh groundwater from a large pond that was present behind the storm berm at this site. This rapid groundwater flow probably drove rapid washout of nitrate, which made it impossible to observe increased nitrate concentrations resulting from nutrient injection. Lower salinity was also observed at some LA015E sample locations in September, probably due to extensive rainfall that occurred before and during collection of these samples. The large error bars associated with the salinity values measured at these sites illustrates the spatial variation (e.g., as a function of depth and horizontal location) at these sites. The salinity at SM006B, on the other hand, was relatively consistent, demonstrating that groundwater flow at this site was primarily tidally driven.

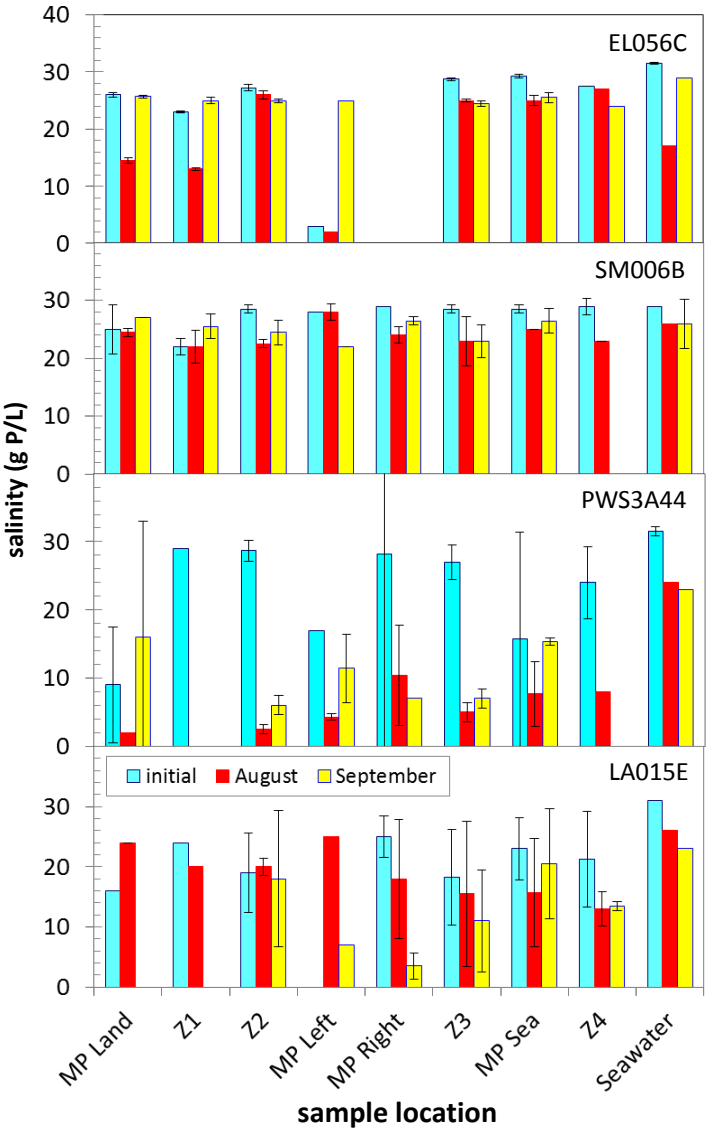

Fig. 17: Salinity observed at multiport (MP) and single-point wells at the bioremediation test sites. Sample locations on the left are most landward and on the right are most seaward.

Conclusions:

Pilot-scale bioremediation systems were installed at four sites in Prince William Sound, Alaska, where lingering oil from the *Exxon Valdez* oil spill was known to persist. Three of these sites (SM006B, PWS3A44, and LA015E) were characterized as shallow-bedrock beaches, meaning that it was not possible to install injection wells to a depth of one meter or greater below the beach surface. Nutrients were injected into the contaminated subsurface under very low pressure and low flow rates ($\leq$0.2 L/min) at these sites. The fourth site (EL056C) was considered to be a deep-bedrock beach, and higher pressures and flow rates (about 1 L/min) were used. These bioremediation systems were operated for less than 7 weeks.

Enhanced biodegradation of PAH compounds was observed at two of the test sites—EL056C and PWS3A44—by comparison of the normalized PAH concentrations observed before

and after startup of the bioremediation systems. The PAH concentrations were normalized to C2-chrysene, a slowly biodegradable PAH that is present at relatively high concentrations in Alaska North Slope crude oil. Reductions in normalized PAH concentrations on the order of 50% were observed at both sites. No effect of bioremediation could be discerned at SM006B or LA015E. It is likely that the relatively slow rates of nutrient injection and slow groundwater flow rates at these sites limited the zone of influence around the injection wells.

This study demonstrated that bioremediation is a feasible response alternative for the lingering oil from the *Exxon Valdez* oil spill, but the extent of remediation that can be achieved and the physical or geomorphological restrictions on the beaches that are amenable to bioremediation must still be defined.

References:

Atlas, R.M. and Bartha, R. 1972. Degradation and mineralization of petroleum in seawater: limitation by nitrogen and phosphorus. Biotechnol. Bioengin. 14: 309-317.

Atlas, R.M. and Bragg, J. 2009. Bioremediation of marine oil spills: when and when not – the *Exxon Valdez* experience. Microb. Biotechnol. 2: 213-221.

Atlas, R. and Bragg, J.R. 2009. Evaluation of PAH depletion of subsurface *Exxon Valdez* oil residues remaining in Prince William Sound in 2007-2008 and their likely bioremediation potential. In: *Proceedings, 32nd AMOP Technical Seminar on Environmental Contamination and Response*, pp. 723-747. Environment Canada, Ottawa, ON, Canada.

Boufadel, M.C., Reeser, P., Suidan, M.T., Wrenn, B.A., Cheng, J., Du, X., and Venosa, A.D. 1999. Optimal nitrate concentration for the biodegradation of n-heptadecane in a variably-saturated sand column. Environ. Technol. 20: 191-199.

Boufadel, M.C., Suidan, M.T., and Venosa, A.D. 2006. Tracer studies in laboratory beach simulating tidal influences. J. Environ. Engin. (ASCE) 132: 616-623.

Boufadel, M.C., Sharifi, Y., Van Aken, B., Wrenn, B.A., and Lee, K. 2010. Nutrient and oxygen concentrations within the sediments of an Alaskan beach polluted with the *Exxon Valdez* oil spill. Environ. Sci. Technol. 44: 7418-7424.

Boufadel, M.C. and Bobo, A.M. 2011. Feasibility of high pressure injection of chemicals into the subsurface for the bioremediation of the *Exxon Valdez* oil. Ground Water Monitor. Remed. 31: 59-67.

Bobo, A., Li, H., and Boufadel, M.C. in press. Groundwater flow in a tidally influenced gravel beach in Prince William Sound, Alaska, J. Hydrol. Engin. (ASCE)

Brovelli, A., Mao, X., and Barry, D.A. 2007. Numerical modeling of tidal influence on density-dependent contaminant transport. Water Resourc. Res. 43: W10426 DOI: 10.1029/2006WR005173

Carls, M.G., Babcock, M.M., Harris, P.M., Irvine, G.V., Cusick, J.A., and Rice, S.D. 2001. Persistence of oiling in mussel beds after the *Exxon Valdez* oil spill. Mar. Environ. Res. 51: 167-190.

Du, X., Reeser, P., Suidan, M.T., Huang, T., Moteleb, M., Boufadel, M.C., and Venosa, A.D. 1999. Optimal nitrate concentration supporting maximum crude oil biodegradation in microcosms. In: *Proceedings, 1999 International Oil Spill Conference*, pp. 485-488. American Petroleum Institute, Washington, DC.

Fiorenza, S. and Ward, C.H. 1997. Microbial adaptation to hydrogen peroxide and biodegradation of aromatic hydrocarbons. J. Ind. Microbiol. Biotechnol. 18: 140-151.

Garcia-Blanco, S. 2004. Testing the resource-ratio theory as a framework for supporting a bioremediation strategy for clean-up of crude oil-contaminated environments. Ph.D. Dissertation, University of Cincinnati, Cincinnati, OH.

Grasshoff, K., Kremling, K., and Ehrhadt, M. 1999. *Methods of Seawater Analysis*. Wiley-VCH, Germany.

Guo, Q., Li., H., Boufadel, M.C., and Sharifi, Y. 2010. Hydrodynamics in a gravel beach and its impact on the *Exxon Valdez* oil spill. J. Geophys. Res., Oceans 115: C12077, doi:10.1029/2010JC006169.

Hayes, M.O. and Michel, J. 1999. Factors determining the long-term persistence of *Exxon Valdez* oil in gravel beaches. Mar. Pollut. Bull. 38: 92-101.

Lawes, B.C. 1990. Soil-induced decomposition of hydrogen peroxide: Preliminary findings. In: *Petroleum Contaminated Soils, Vol. 3*, pp. 239-249. Kostecki, P.T. and Calabrese, E.J. (Eds.). Lewis Publishers, Inc. Chelsea, MI.

Li, H., Venosa, A.D., and Boufadel, M.C. 2007. A universal nutrient application strategy for the bioremediation of oil polluted beaches. Mar. Pollut. Bull. 54: 1146-1161.

Li, H. and Boufadel, M.C. 2010. Long-term persistence of oil from the *Exxon Valdez* spill in two-layer beaches. Nature Geosci. 3: 96-99.

Michel, J. and Hayes, M.O. 1999. Weathering patterns of oil residues eight years after the *Exxon Valdez* oil spill. Mar. Pollut. Bull. 38: 855-863.

Neff, J.M., Owens, E.H., Stoker, S.W., and McCormick, D.M. 1995. Shoreline oiling conditions in Prince William Sound following the *Exxon Valdez* oil spill. In: Wells, P.G., Butler, J.N., and Hughes, J.S., (Eds.), *Exxon Valdez Oil Spill: Fates and Effects in Alaskan Waters.* STP 1219. American Society for Testing and Materials, Philadelphia, PA, pp 312–346.

Neff, J.M. and Stubblefield, W.A.1995. Chemical and toxicological evaluation of water quality following the *Exxon Valdez* oil spill. In: Wells, P.G., Butler, J.N., and Hughes, J.S., (Eds.), *Exxon Valdez Oil Spill: Fates and Effects in Alaskan Waters.* STP 1219. American Society for Testing and Materials, Philadelphia, PA, pp. 141-177.

Oxmann, J.F., Pham, Q.H., and Lara, R.J. 2008. Quantification of individual phosphorus species in sediment: a sequential conversion and extraction method. Eur. J. Soil Sci. 59: 1177-1190.

Page, D.S., Boehm, P.D., and Neff, J.M. 2008. Shoreline type and subsurface oil persistence in the *Exxon Valdez* spill zone of Prince William Sound, Alaska. In: *Proceedings, 31st AMOP Technical Seminar on Environmental Contamination and Response*, pp. 545-563. Environment Canada, Ottawa, ON, Canada.

Pardieck, D.L., Bouwer, E.J., and Stone, A.J. 1992. Hydrogen peroxide use to increase oxidant capacity for *in situ* bioremediation of contaminated soils and aquifers: A review. J. Cont. Hydrol. 9: 221-242.

Seal Analytical. 2008. *Autoanalyzer3 User Guide*. Seal Analytical, Mequon, WI.

Sharifi, Y., Van Aken, B., and Boufadel, M.C. 2011. The effect of pore water chemistry on the biodegradation of the *Exxon Valdez* oil spill. Water Qual. Expo. Health 2: 157-168.

Short, J.W., and Heintz, R.A. 1997. Identification of *Exxon Valdez* oil in sediments and tissues from Prince William Sound and the northwestern Gulf of Alaska based on a PAH weathering model. Environ. Sci. Technol. 31: 2375-2384.

Short, J.W., Lindeber, M.R., Harris, P.M., Maselko, J.M., Pella, J.J., and Rice, S.D. 2004. Estimate of oil persisting on the beaches of Prince William Sound 12 years after the *Exxon Valdez* oil spill. Environ. Sci. Technol. 38: 19-25.

Short, J.W., Maselko, J.M., Lindeberg, M.R., Harris, P.M., and Rice, S.D. 2006. Vertical distribution and probability of encountering intertidal *Exxon Valdez* oil on shorelines of three embayments within Prince William Sound, Alaska. Environ. Sci. Technol. 40: 3723-3729.

Smith, V.H., Graham, D.W., and Cleland, D.D. 1998. Application of resource-ratio theory to hydrocarbon biodegradation. Environ. Sci. Technol. 32: 3386-3395.

Spain, J.C., Milligan, J.D., Downey, D.C., and Slaughter, J.K. 1989. Excessive bacterial decomposition of H_2O_2 during enhanced biodegradation. Ground Water 27: 163-167.

Taylor, E. and Reimer, D. 2008. Oil persistence on beaches in Prince William Sound – A review of SCAT surveys conducted from 1989 to 2002. Mar. Pollut. Bull. 56: 458-474.

Tiyapongpattana, W., Pongsakul, P., Shiowatana, J., and Nacapricha, D. 2004. Sequential extraction of phosphorus in soil and sediment using a continuous-flow system. Talanta 62: 765-771.

Venosa, A.D., Suidan, M.T., Wrenn, B.A., Strohmeier, K.L., Haines, J., Eberhart, B.L., King, D., and Holder, E. 1996. Bioremediation of an experimental oil spill on the shoreline of Delaware Bay. Environ. Sci. Technol. 30: 1764-1775.

Venosa, A.D., Campo, P., and Suidan, M.T. 2010. Biodegradability of lingering crude oil 19 years after the *Exxon Valdez* oil spill. Environ. Sci. Technol. 44: 7613-7621.

Xia, Y., Li., H., and Boufadel, M.C. 2010. Factors affecting the persistence of the Exxon Valdez oil on a shallow bedrock beach. Water Resour. Res. 46: W10528, 17 pp., doi:10.1029/2010WR009179